European Journal of Inorganic Chemistry

Supporting Information

N,N,O Pincer Ligand with a Deprotonatable Site That Promotes Redox-Leveling, High Mn Oxidation States, and a Mn_2O_2 Dimer Competent for Catalytic Oxygen Evolution

Hannah M. C. Lant, Thoe K. Michaelos, Liam S. Sharninghausen, Brandon Q. Mercado, Robert H. Crabtree,* and Gary W. Brudvig*

ejic201801343-sup-0001-SupMat.pdf

Table of Contents:

1. Synthesis, Characterization, and Electrochemical Measurements of 1-5.

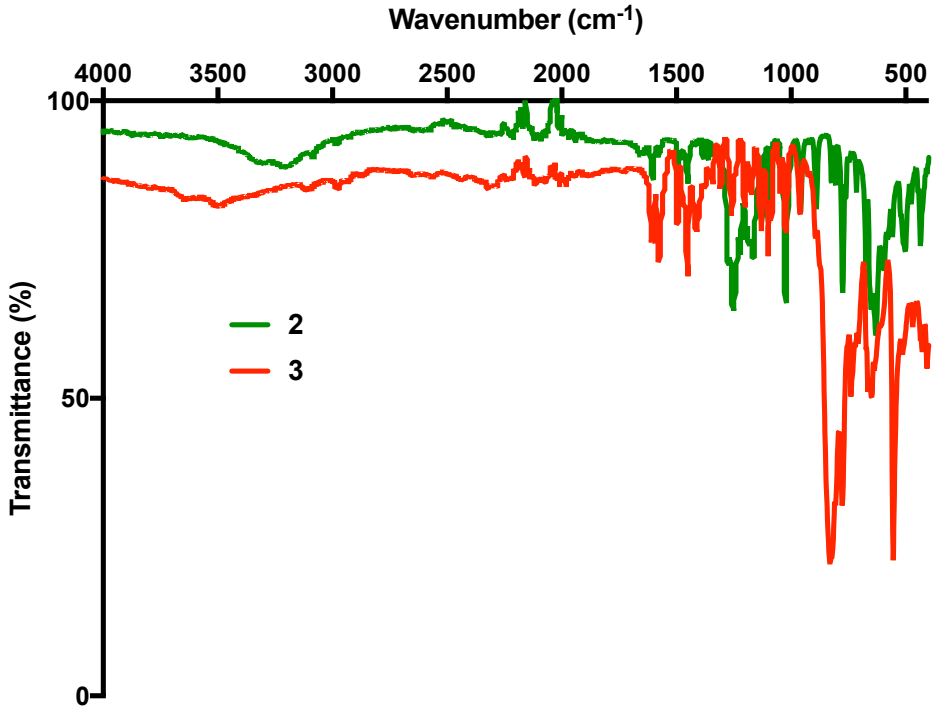

Figure S1. IR spectra of **2**, and **3**.

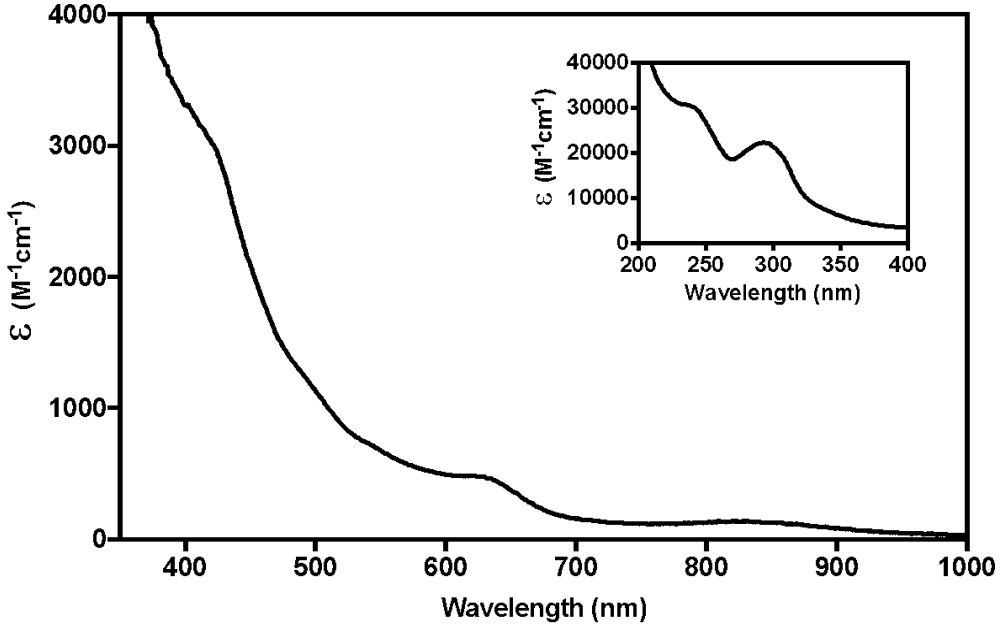

Figure S2. UV-visible spectrum of **2** in MeCN, with inset showing peaks in the UV region. Concentration of solution showing visible features is 4.76 x10^{-4} M, where the solution for the inset is 1.76 x 10^{-5} M.

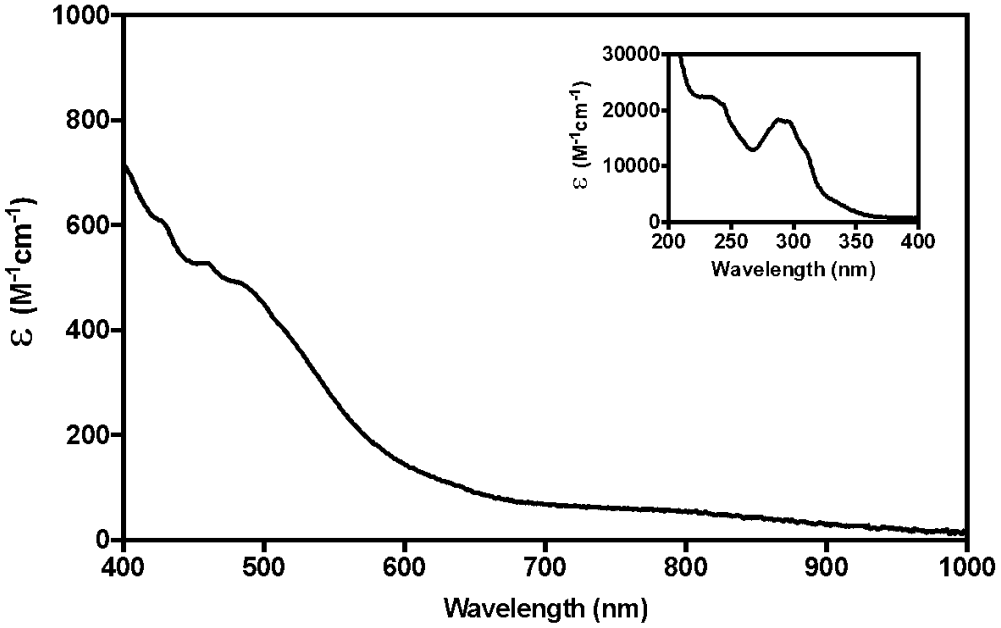

Figure S3. UV-visible spectrum of **3** in MeCN, with inset showing peaks in the UV region. Concentration of solution showing visible features is 6.13 x10^{-4} M, where the solution for the inset is 2.27 x 10^{-5} M.

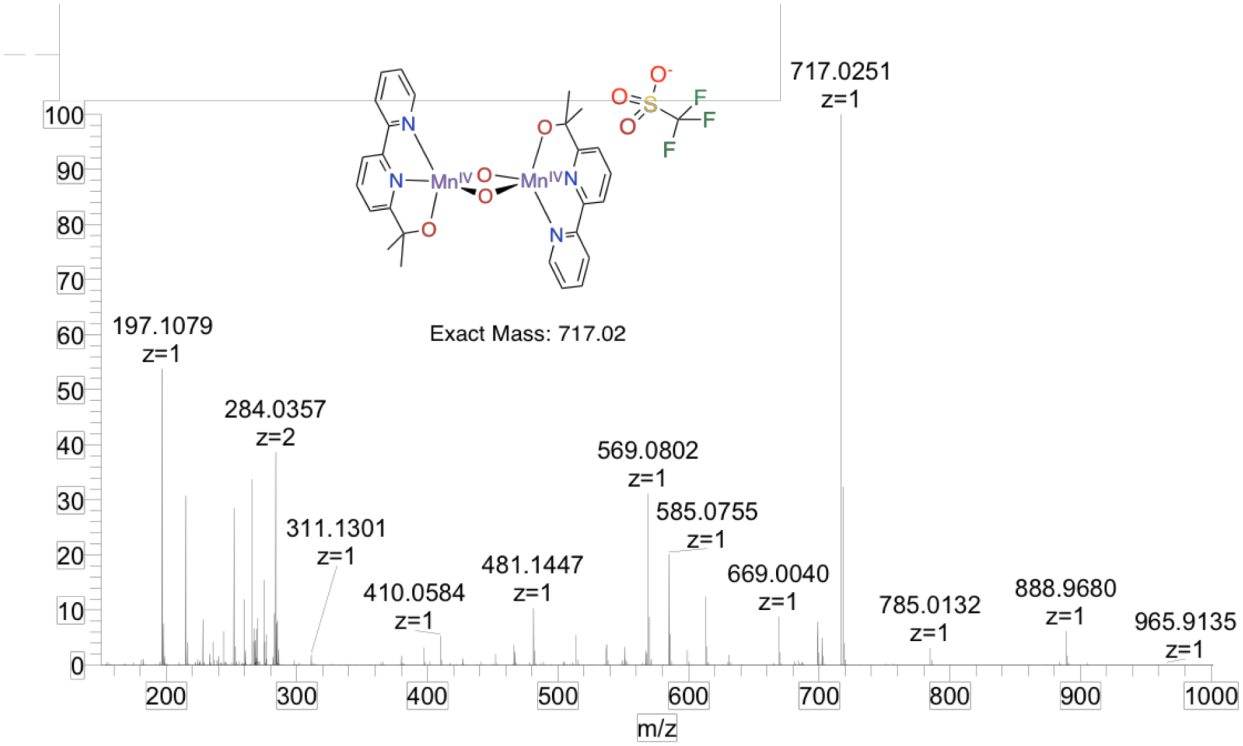

Figure S4. Mass spectrum of **2**. The complex, which is observed as a monocation with one triflate counterion but no water ligands, appears to desolvate upon injection into the instrument, as is commonly observed with water-ligated $Mn_2(\mu\text{-}O)_2$ and $Mn_4(\mu\text{-}O)_5$ complexes.[1,2,3]

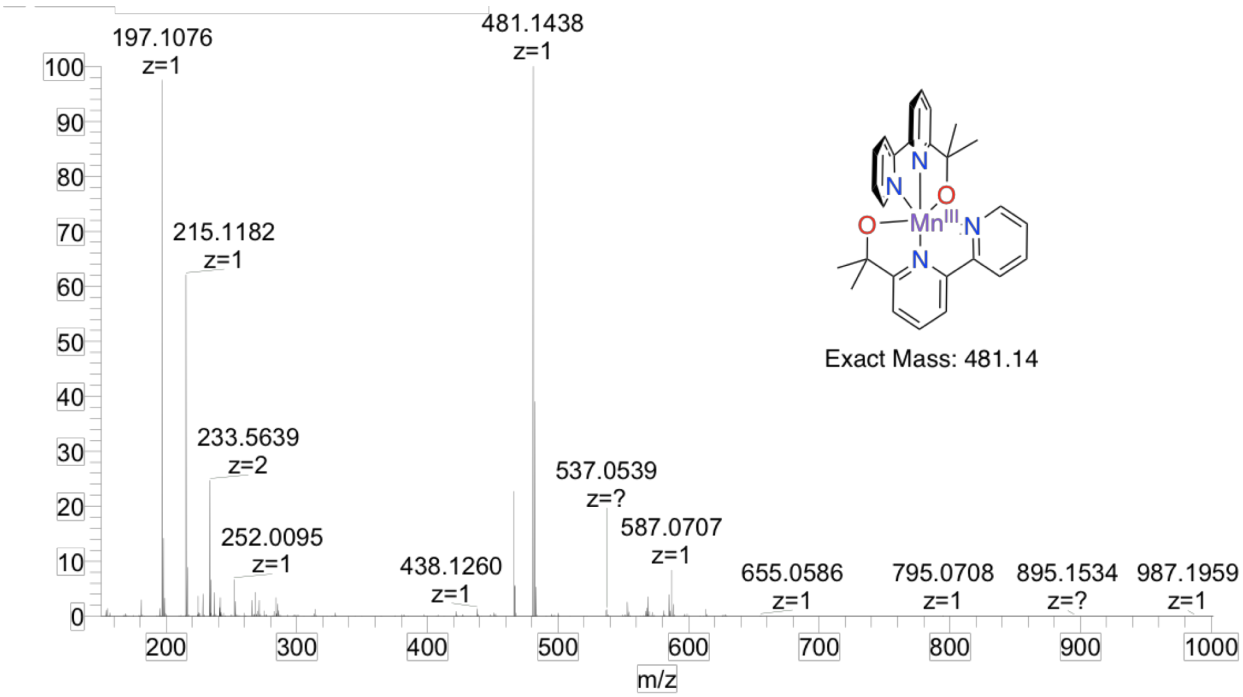

Figure S5. Mass spectrum of **3**. The complex, which is observed as a monocation appears to lose the proton on the bipyalk ligand.

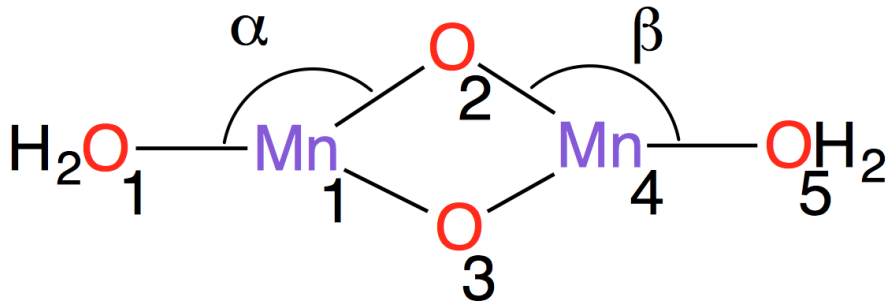

Figure S6. *Cis* versus *trans* geometry of waters for dimers of the type $[Mn_2(\mu\text{-}O)_2(L)_2(H_2O)_2]$ documented in the Cambridge Crystallographic Database, tabulated in Table 1.

Table S1. Results from a search in the Cambridge Crystallographic Database for $Mn_2(\mu\text{-}O)_2$ dimers. Note that all results except **2** feature a trans geometry of bound waters at each Mn center, and all but **2** are isolated and crystallized in the $Mn_2^{III,IV}$ state.

[a] Dimer crystallizes in P-1 spacegroup, but inversion center is not found within the diamond core.
[b] Dimer crystallizes in P-1 spacegroup, features inversion center in the center of diamond such that manganese atoms are crystallographically equivalent.
[c] Dimer crystallizes in $P2_1/c$ spacegroup, but inversion center is not found within the diamond core.
[d] Dimer crystallizes in $P2_1/c$ spacegroup, features inversion center in the center of diamond such that manganese atoms are crystallographically equivalent.

Entry:	**Compound:**	**CCDC Code:**	**Ref:**	α, β °
1.	$[(OH_2)(PrO\text{-}terpy)Mn^{III}(\mu\text{-}O)_2Mn^{IV}(PrO\text{-}terpy)(OH_2)]^{3+}$	[a]DAPQIW	1	94.93, 189.34
	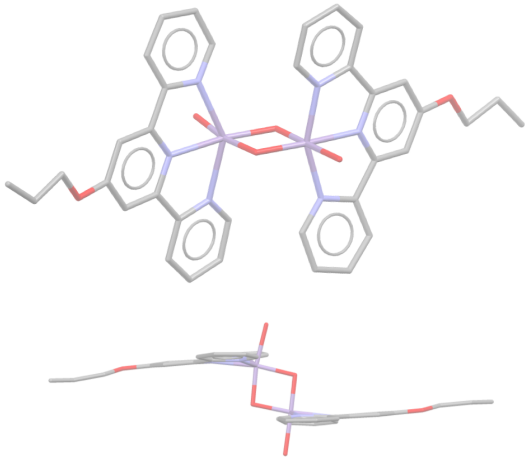			
2.	$(OH_2)(Me\text{-}terpy)Mn^{III}(\mu\text{-}O)_2Mn^{IV}(Me\text{-}terpy)(OH_2)]^{3+}$	[b]DAPQOC	4	93.28, 185.08
	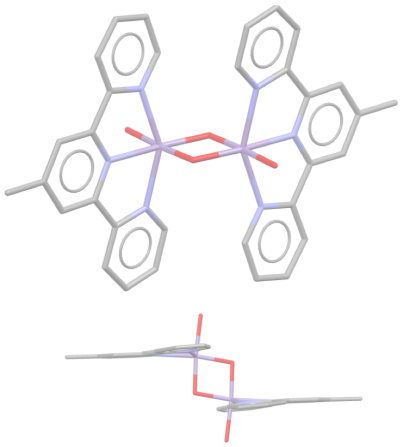			
3.	$(OH_2)(MeS\text{-}terpy)Mn^{III}(\mu\text{-}O)_2Mn^{IV}(MeS\text{-}terpy)(OH_2)]^{3+}$	[b]DAPQUI	1	91.72, 185.57

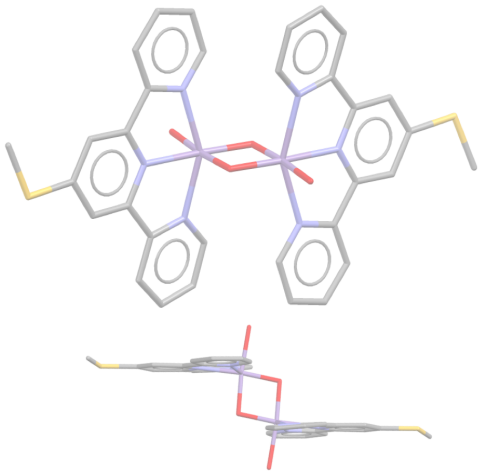

4.	$(OH_2)(MeO\text{-}terpy)Mn^{III}(\mu\text{-}O)_2Mn^{IV}(MeO\text{-}terpy)(OH_2)]^{3+}$	[c]DAPRAP	1	95.12, 192.45

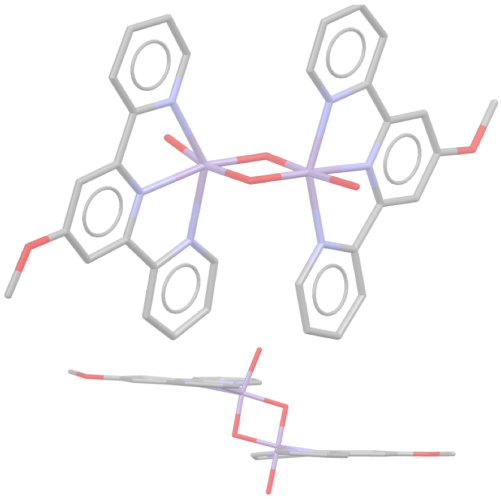

5.	$[(OH_2)(EtO\text{-}terpy)Mn^{III}(\mu\text{-}O)_2Mn^{IV}(EtO\text{-}terpy)(OH_2)]^{3+}$	[b]DAPRET	1	91.94, 185.59

6.	$(OH_2)(BuO\text{-}terpy)Mn^{III}(\mu\text{-}O)_2Mn^{IV}(BuO\text{-}terpy)(OH_2)]^{3+}$	[b]DAPRIX	1	94.27, 183.65

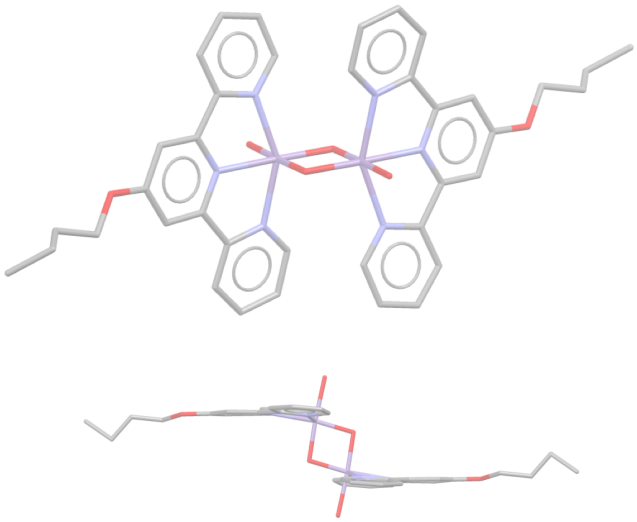

7.	$(OH_2)(terpy)Mn^{III}(\mu\text{-}O)_2Mn^{IV}(terpy)(OH_2)]^{3+}$	[b]FIQFIU	2	94.08, 183.45

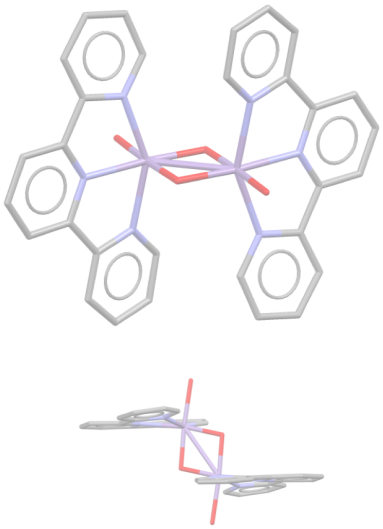

8.	(OH_2)(Py-terpy)$Mn^{III}(\mu\text{-}O)_2Mn^{IV}$(Py-terpy)$(OH_2)]^{3+}$	[d]GETTOQ	3	93.43, 184.11

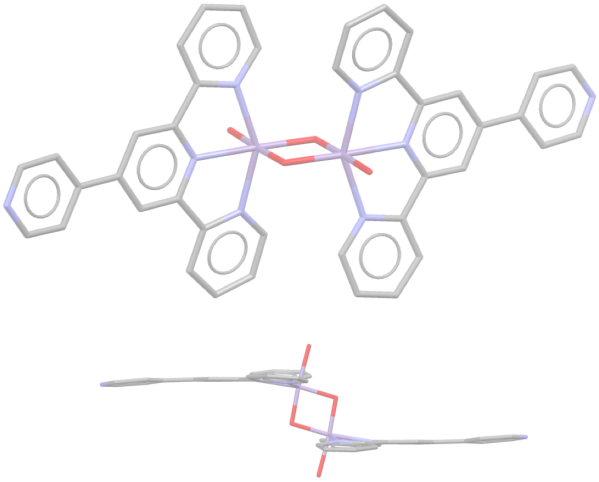

9.	(OH_2)(*mes*-terpy)$Mn^{III}(\mu\text{-}O)_2Mn^{IV}$(*mes*-terpy)$(OH_2)]^{3+}$	[a]XAYCAC	1	93.49, 184.72

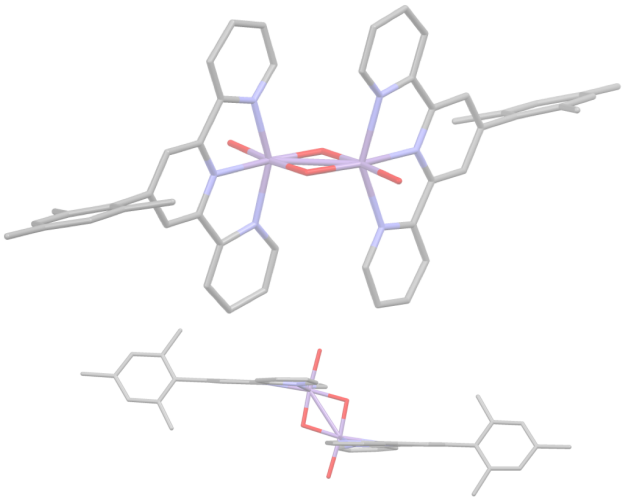

10.	$(OH_2)(bipyalk)Mn^{IV}(\mu\text{-}O)_2Mn^{IV}(bipyalk)(OH_2)]^{3+}$	[a]	This work	92.92, 93.30

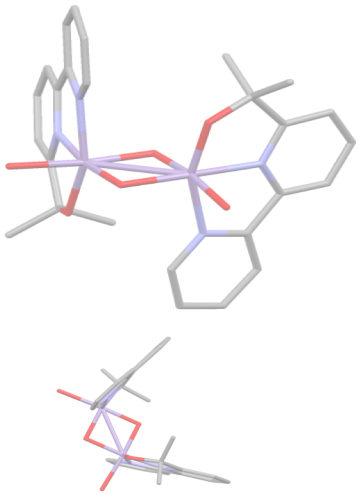

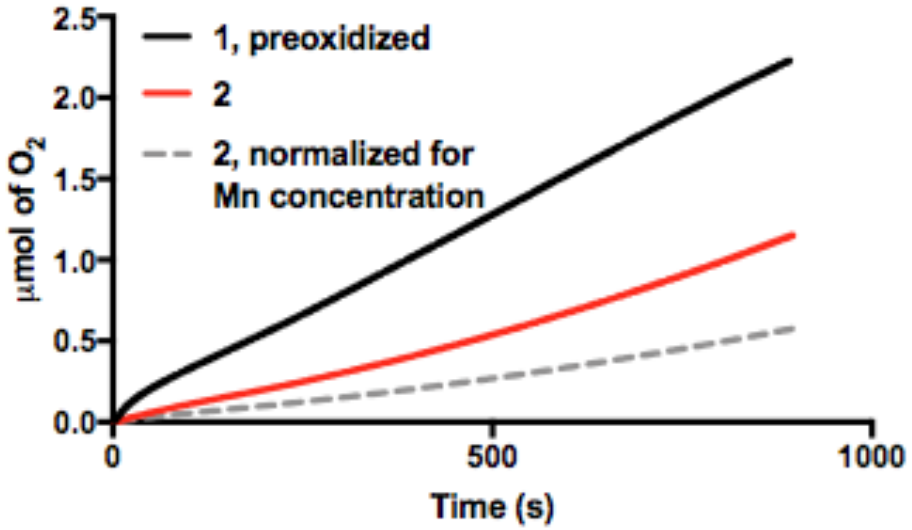

Figure S7. Typical oxygen-evolution trace. **2**, red, (50 µM) is injected into Clark electrode at t = 0 containing solution of 10 mM $KHSO_5$. This is compared against a typical oxygen evolution trace observed when **1** is "preoxidized" in a concentrated solution of $KHSO_5$ prior to being injected into a solution of 10 mM $KHSO_5$ sacrificial oxidant in the Clark electrode chamber such that the final concentration is 50 µM. The dotted grey line shows the oxygen evolution trace of **2** with product oxygen values divided by two to normalize for total Mn content.

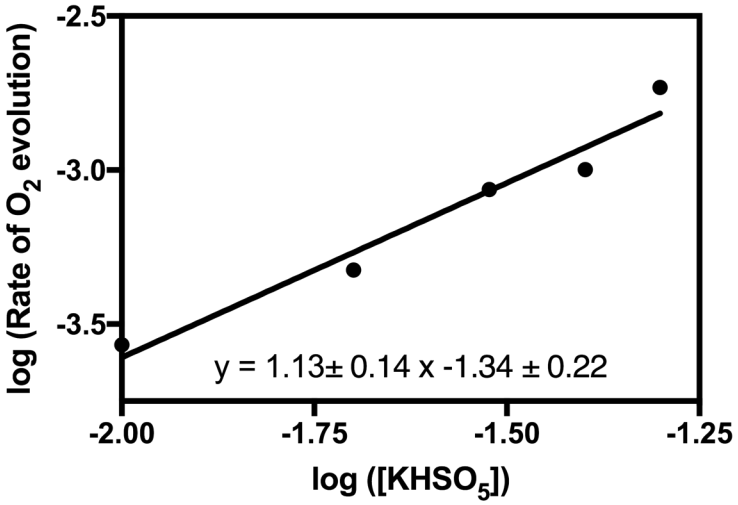

Figure S8. Logarithmic plot of dependence of rate of O_2 evolution on [$KHSO_5$], where [**2**] = 50 µM.

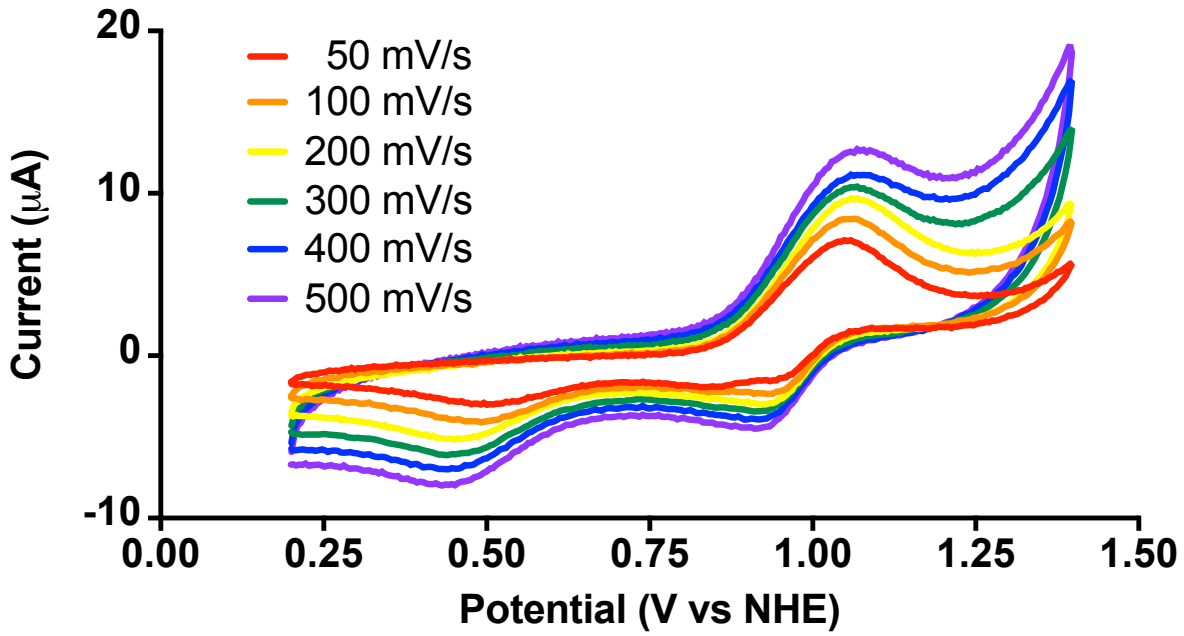

Figure S9. Scan rate dependence on CVs of **1**. Conditions: 2.5 mM in 0.1 M acetate buffer at pH 4.47, GC working electrode, Pt wire counter electrode, Ag/AgCl reference electrode.

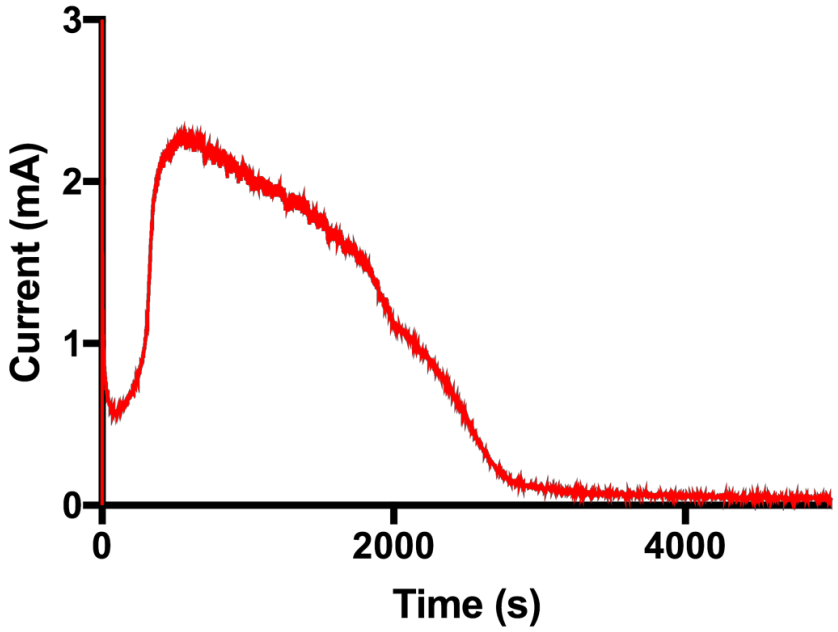

Figure S10. Bulk electrolysis at 1.2 V vs. NHE of **1** (2.0 mM) in 0.1 M acetate buffer at pH 4.47 with a platinum basket working electrode, platinum mesh counter electrode, and Ag/AgCl reference electrode. Integrated charge passed is 4.05 C or 2.50 10^{19} e^-. For a two-electron oxidation at this concentration, theoretical number of electrons passed is 2.54 x 10^{19} e^-.

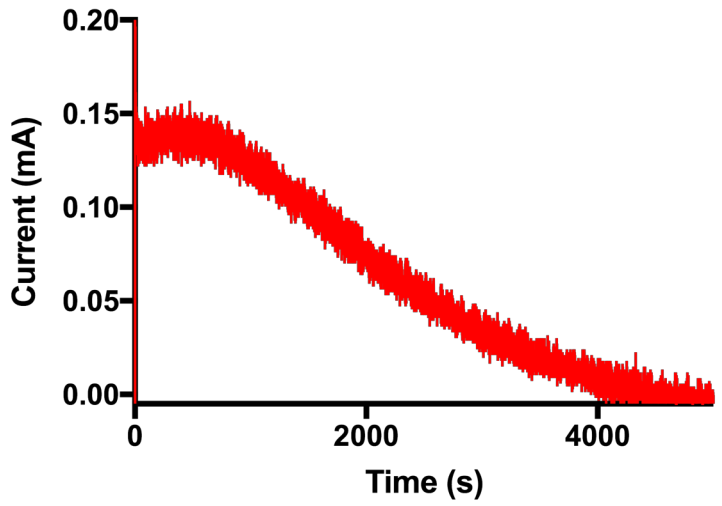

Figure S11. Bulk electrolysis at 930 mV vs. NHE of **1** (1.0 mM) in 0.1 M acetate buffer at pH 4.47 with a platinum basket working electrode, platinum mesh counter electrode, and Ag/AgCl reference electrode. Integrated charge passed is 1.078 C or 6.73 x 10^{18} e^-. For a one-electron oxidation at this concentration, theoretical number of electrons passed is 1.15 x 10^{19} e^-.

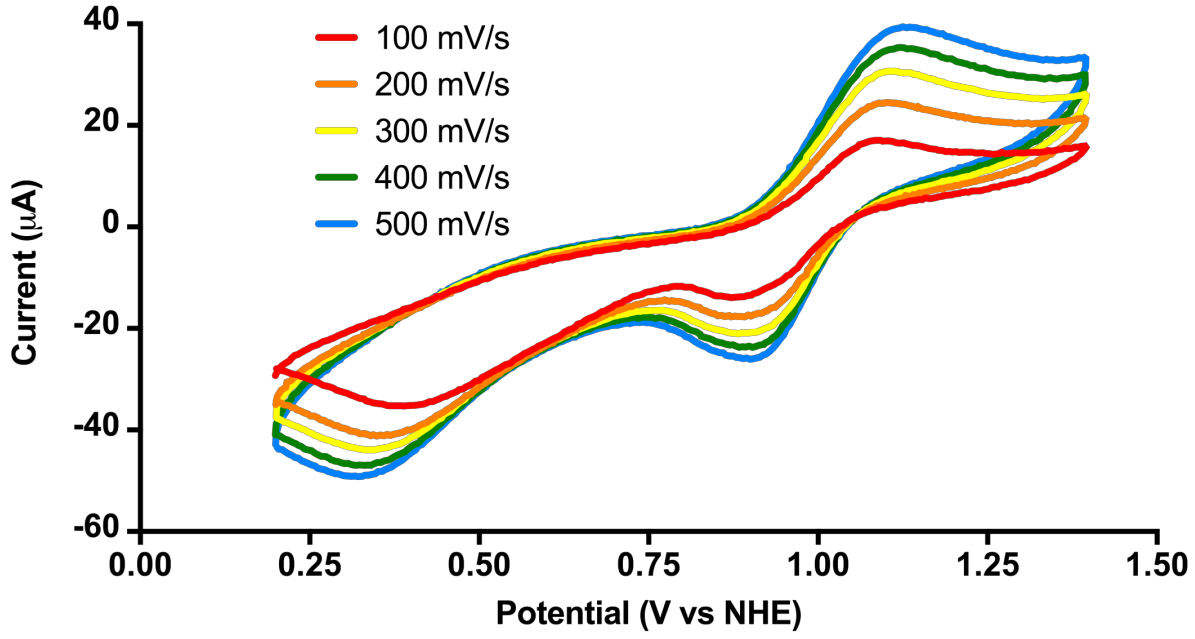

Figure S12. Scan rate dependence on CVs of **2**. Conditions: 2.5 mM in 0.1 M acetate buffer at pH 4.47, GC working electrode, Pt wire counter electrode, Ag/AgCl reference electrode.

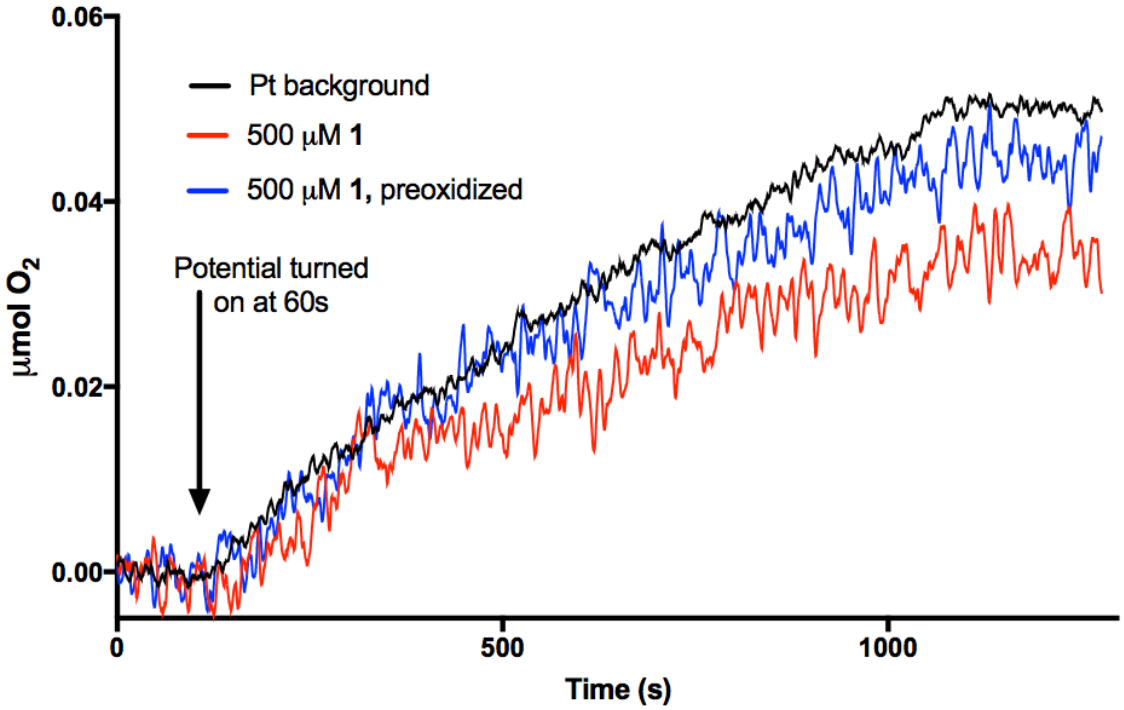

Figure S13. Sample O_2 evolution traces from Clark electrode from attempts to probe for electrocatalytic water-oxidation activity of **1** showing no O_2 evolution was observed over background levels. A stock solution of complex, pretreated with 2 equivalents of $KHSO_5$ in the blue trace, was injected into the Clark electrode chamber at time = 0 sec such that the final concentration was 500 μM. Potential was applied at time = 60 s. Conditions: Pt working electrode, Ag/AgCl reference electrode, Pt wire counter electrode, 0.1 M K_2SO_4 at 1.6 V applied potential vs. NHE. Other conditions assayed included potentials ranging from 1.2 V to 1.8 V, use of glassy carbon working electrode, and 0.1 M acetate buffer. Similar results were seen in other cases, and no O_2 was observed above background levels in any case.

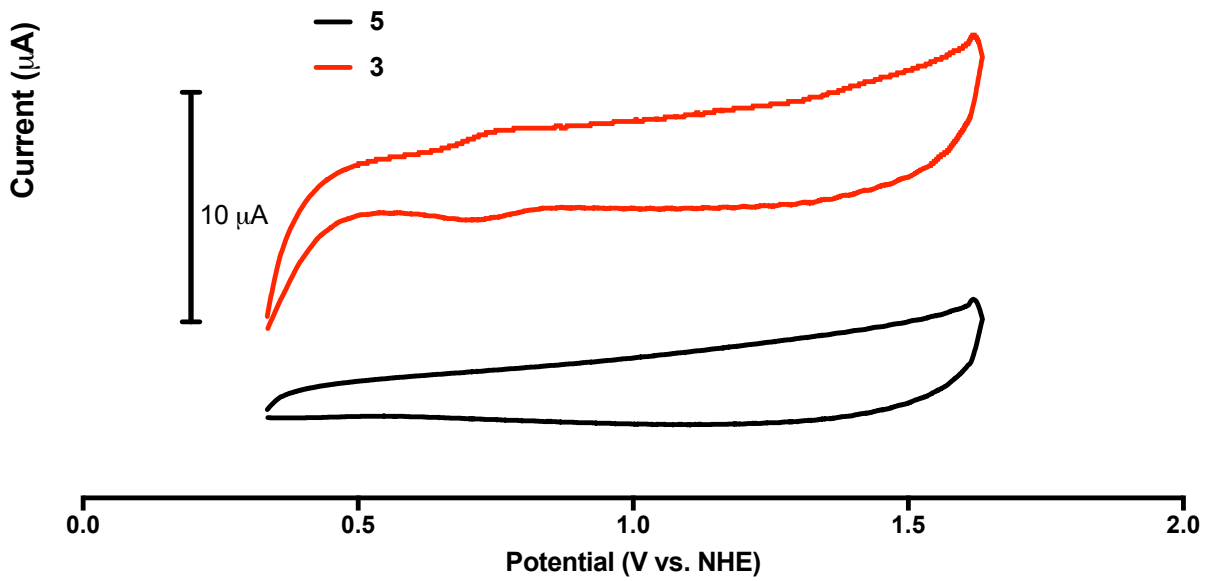

Figure S14. CV of **5** and **3**. Conditions: 2.5 mM in 0.1 M $tBuN_4PF_6$ at in MeCN. GC working electrode, Pt wire counter electrode, Ag wire pseudo reference electrode, referenced against an internal ferrocene standard to express as NHE.

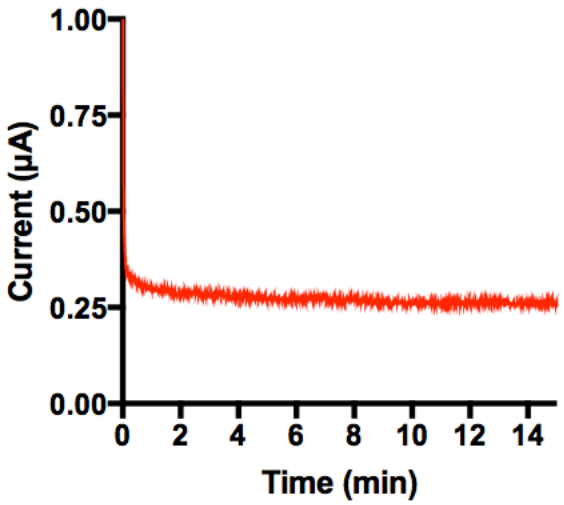

Figure S15. Sample chronoamperogram from spectroelectrochemical experiments. Current plateau by the end of the experiment indicates equilibrium at the applied potential has been reached. The sample CA above is from an electrolysis of 3 as shown in Fig. S17 above at 2.5 mM in a 0.1 M NBu_4PF_6/MeCN solution at the intermediate potential of 1.05 V for 15 minutes.

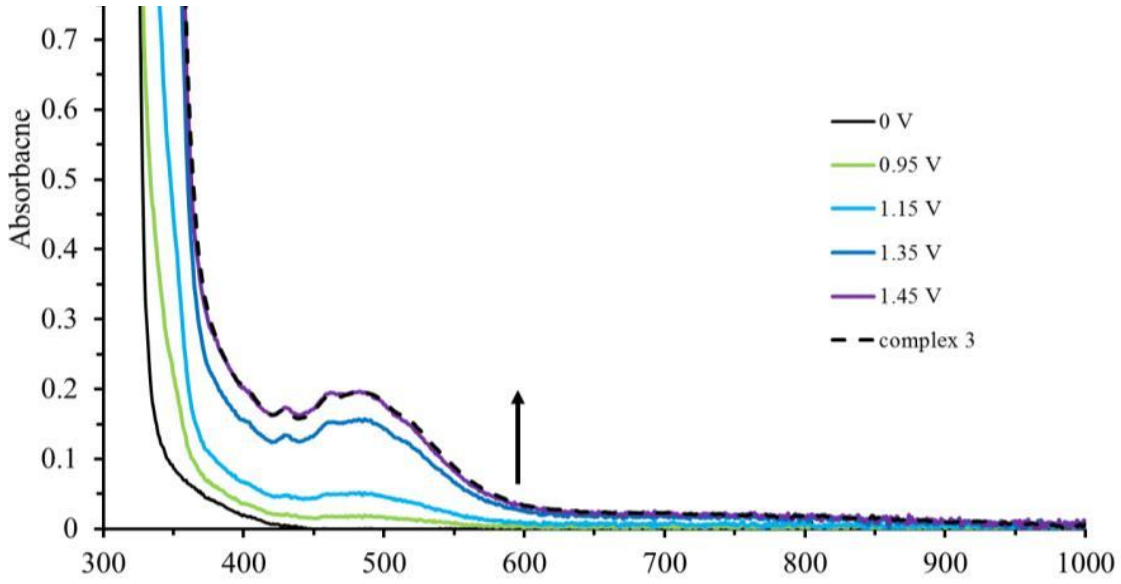

Figure S16. Spectroelectrochemistry of **5** (2.5 mM) in a 0.1 M NBu_4PF_6/MeCN solution. Potentials were applied for 15 minutes each in increasingly oxidizing steps as indicated. The dashed line shows a normalized spectrum of **3** for comparison.

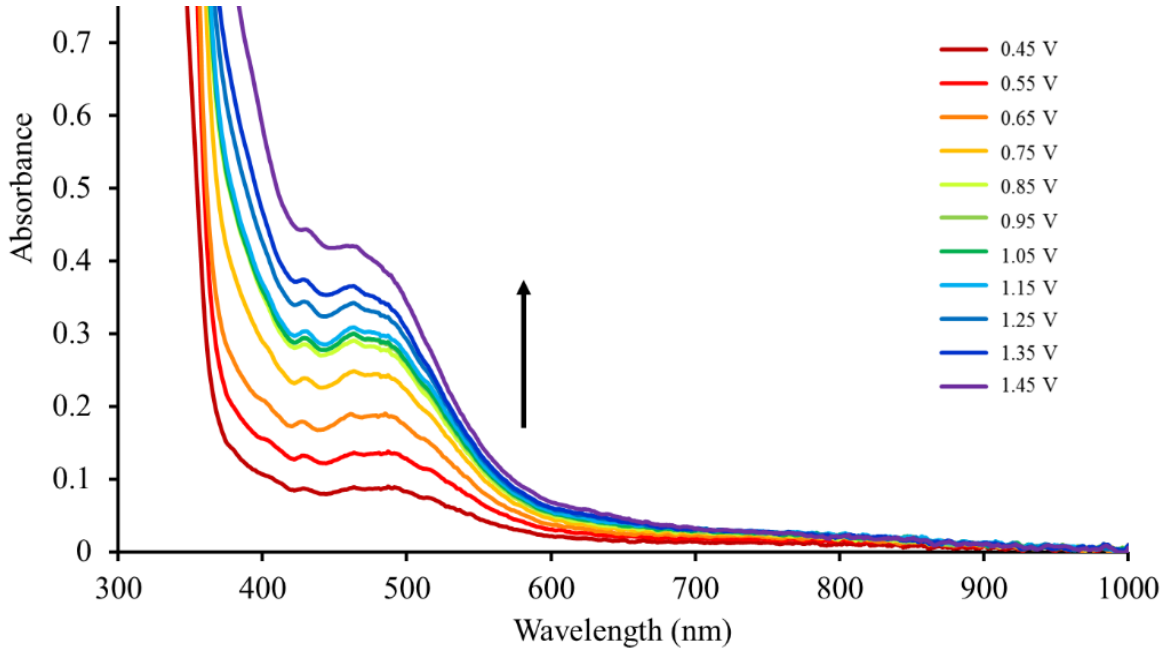

Figure S17. Spectroelectrochemistry of **3** (2.5 mM) in a 0.1 M NBu_4PF_6/MeCN solution. Potentials were applied for 15 minutes each in increasingly oxidizing steps as indicated.

2. Crystallographic Information:

2.1 Experimental:
Low-temperature diffraction data (ω-scans) were collected on a Rigaku SCX Mini diffractometer coupled to a Rigaku Mercury275R CCD for structure **2** with Mo Kα radiation (λ = 0.71073 Å). Similar data were collected on a Rigaku MicroMax-007HF diffractometer coupled to a Saturn994+ CCD detector with Cu Kα (λ = 1.54178 Å) for the structures **3** and **4**. The diffraction images were processed and scaled using CrystalClear 2.0 r15 for **2** and **4**; Rigaku Oxford Diffraction ver. 1.171.39.16b for **3**. The structures were solved with SHELXT and were refined against F^2 on all data by full-matrix least squares with SHELXL. All non-hydrogen atoms were refined anisotropically. Unless stated otherwise, hydrogen atoms were first found in the difference map and then included in the model at geometrically calculated positions and refined using a riding model. The isotropic displacement parameters of all hydrogen atoms were fixed to 1.2 times the U value of the atoms to which they are linked (1.5 times for methyl groups). The full numbering scheme of **2** - **4** can be found in the full details of the X-ray structure determination (CIF), which are included as Supporting Information. CCDC files 1872330(**2**), 1872331 (**3**), and 1872332 (**4**) contain the supplementary crystallographic data for this paper. These data can be obtained free of charge from The Cambridge Crystallographic Data Center via www.ccdc.cam.ac.uk/data_request/cif.

2.2 Details for Diffraction and Refinement for **2**.

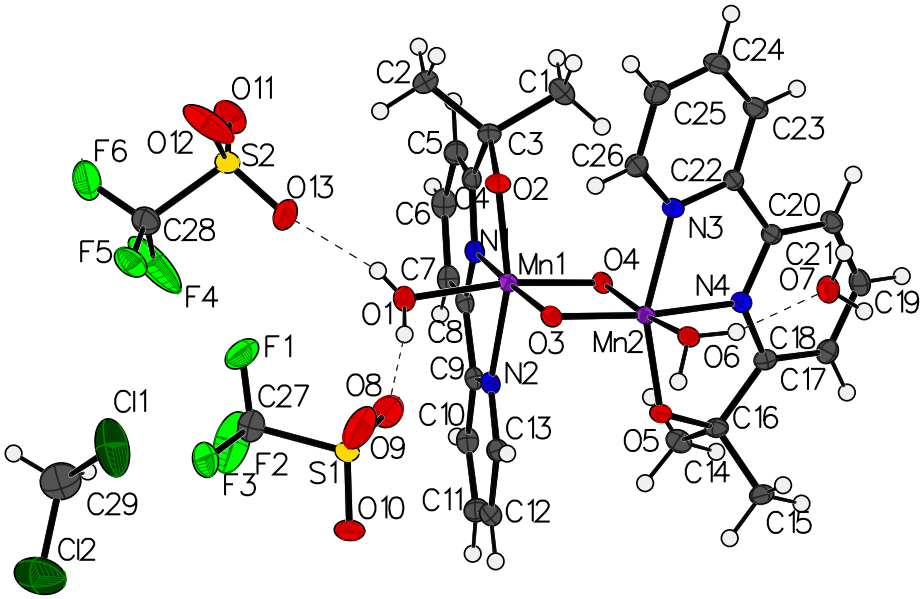

Figure S18. Thermal ellipsoid diagram for **2** with complete numbering scheme. Thermal ellipsoids are displayed at the 50% probability level.

Table S2. Hydrogen bonds for **2** [Å and °].

D-H...A	d(D-H)	d(H...A)	d(D...A)	<(DHA)
O(1)-H(1B)...O(8)	0.82(4)	1.80(4)	2.617(3)	176(4)
O(1)-H(1A)...O(13)	0.74(4)	2.00(4)	2.690(3)	156(4)
O(6)-H(6B)...O(5)#1	0.77(4)	1.95(4)	2.709(3)	171(4)
O(6)-H(6A)...O(7)	0.81(5)	1.88(5)	2.667(3)	164(4)
O(7)-H(7B)...O(10)#1	0.75(4)	2.10(4)	2.851(3)	173(4)
O(7)-H(7A)...O(12)#2	0.75(5)	2.00(5)	2.748(3)	174(4)

Symmetry transformations used to generate equivalent atoms:
#1 -x+1,-y+1,-z+2 #2 -x+2,-y+1,-z+2

Table S3. Crystal data and structure refinement for **2**.

Identification code	mini-16006	
Empirical formula	C14.50 H17 Cl F3 Mn N2 O6.50 S	
Formula weight	502.75	
Temperature	93(2) K	
Wavelength	0.71075 Å	
Crystal system	Triclinic	
Space group	P-1	
Unit cell dimensions	a = 11.2035(3) Å	a= 96.6660(19)°.
	b = 13.6612(3) Å	b= 107.783(2)°.
	c = 14.3304(3) Å	g = 107.945(2)°.
Volume	1932.70(9) $Å^3$	
Z	4	
Density (calculated)	1.728 Mg/m^3	
Absorption coefficient	0.996 mm^{-1}	
F(000)	1020	
Crystal size	0.200 x 0.200 x 0.200 mm^3	
Crystal color and habit	Green Block	
Diffractometer	Rigaku Mercury275R CCD	
Theta range for data collection	1.950 to 26.388°.	
Index ranges	-13<=h<=13, -17<=k<=17, -17<=l<=17	
Reflections collected	31014	
Independent reflections	7858 [R(int) = 0.0229]	
Observed reflections (I > 2sigma(I))	6986	
Completeness to theta = 25.242°	99.8 %	
Absorption correction	Semi-empirical from equivalents	
Max. and min. transmission	1.00000 and 0.97097	
Solution method	SHELXT-2014/5 (Sheldrick, 2014)	
Refinement method	SHELXL-2014/7 (Sheldrick, 2014)	
Data / restraints / parameters	7858 / 0 / 657	
Goodness-of-fit on F^2	1.042	
Final R indices [I>2sigma(I)]	R1 = 0.0408, wR2 = 0.0982	
R indices (all data)	R1 = 0.0477, wR2 = 0.1032	

Extinction coefficient	n/a
Largest diff. peak and hole	1.260 and -1.603 e.Å^{-3}

2.3 Details for Diffraction and Refinement for **3**.

Refinement Details:
In the DCM solvent molecule, Cl1 is disordered over two positions (40:60). A rigid body (RIGU) restraint was used for Cl1A, C27, Cl2 and Cl1B, C27, Cl2 with sigma for 1-2 distances of 0.004 Å and sigma for 1-3 distances of 0.004 Å. For the DCM molecule, hydrogen atoms were generated with respect to the disordered riding atoms.

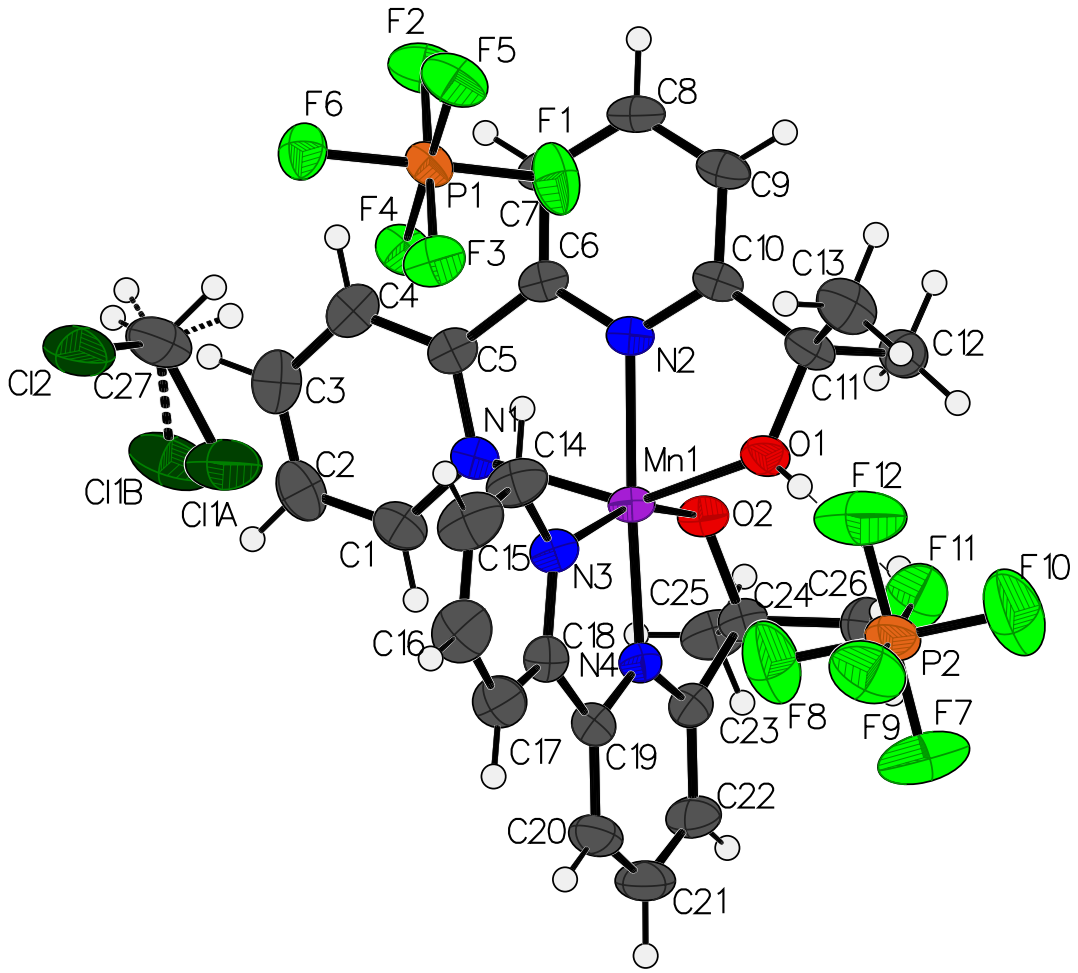

Figure S19. Thermal ellipsoid diagram for **3** with complete numbering scheme. Thermal ellipsoids are displayed at the 50% probability level.

Table S4. Crystal data and structure refinement for **3**.

Identification code	007-15137

Empirical formula	C27 H29 Cl2 F12 Mn N4 O2 P2	
Formula weight	857.32	
Temperature	293(2) K	
Wavelength	1.54184 Å	
Crystal system	Triclinic	
Space group	P-1	
Unit cell dimensions	a = 10.3726(4) Å	a= 85.762(3)°.
	b = 13.0872(5) Å	b= 85.181(3)°.
	c = 13.7851(5) Å	g = 67.805(3)°.
Volume	1724.72(12) $Å^3$	
Z	2	
Density (calculated)	1.651 Mg/m^3	
Absorption coefficient	6.327 mm^{-1}	
F(000)	864	
Crystal size	0.1 x 0.1 x 0.05 mm^3	
Crystal color and habit	Red Plate	
Diffractometer	Rigaku MicroMax-007HF	
Theta range for data collection	3.221 to 66.991°.	
Index ranges	-12<=h<=12, -15<=k<=15, -16<=l<=16	
Reflections collected	60764	
Independent reflections	6046 [R(int) = 0.0579]	
Observed reflections (I > 2sigma(I))	5847	
Completeness to theta = 66.991°	98.1 %	
Absorption correction	Semi-empirical from equivalents	
Max. and min. transmission	1.00000 and 0.71781	
Solution method	SHELXT-2014/5 (Sheldrick, 2014)	
Refinement method	SHELXL-2014/7 (Sheldrick, 2014)	
Data / restraints / parameters	6046 / 15 / 469	
Goodness-of-fit on F^2	1.050	
Final R indices [I>2sigma(I)]	R1 = 0.0404, wR2 = 0.1032	
R indices (all data)	R1 = 0.0415, wR2 = 0.1040	
Extinction coefficient	n/a	
Largest diff. peak and hole	0.667 and -0.614 e.$Å^{-3}$	

Table S5. Hydrogen bonds for 007-15137 [Å and °].

D-H...A	d(D-H)	d(H...A)	d(D...A)	<(DHA)
O(1)-H(1)...F(11)	0.65(4)	2.14(4)	2.788(3)	175(5)

2.4 Details for Diffraction and Refinement for **4**.

Refinement Details:

Both PF_6 groups are disordered over 2 positions. The disordered positions were first refined independently of each other. The site occupancies of the major and minor components of each PF_6 were found to be nearly identical and were subsequently linked by the same free variable. The four sets of atoms which make up the disordered models are: {P1 F1 F2A F3A F4A F5A F6A}, {P1 F1 F2B F3B F4B F5B F6B}, {P2 F7 F8A F9A F10A F11A F12}, {P2 F7 F8B F9B F10B F11B F12}. The atoms of the major and minor components were distinguished with the suffixes "A" and "B", where their site occupancy factors refined to values of 0.70(1) and 0.30(1), respectively. The program SQUEEZE was used to compensate for the contribution of disordered solvents contained in voids within the crystal lattice from the diffraction intensities. This procedure was applied to the data file and the submitted model is based on the solvent removed data. Based on the total electron density found in the voids (18.6 e/Å^3), it is likely that ~2 water molecules are present in the unit cell. See "_platon_squeeze_details" in the CIF for more information.

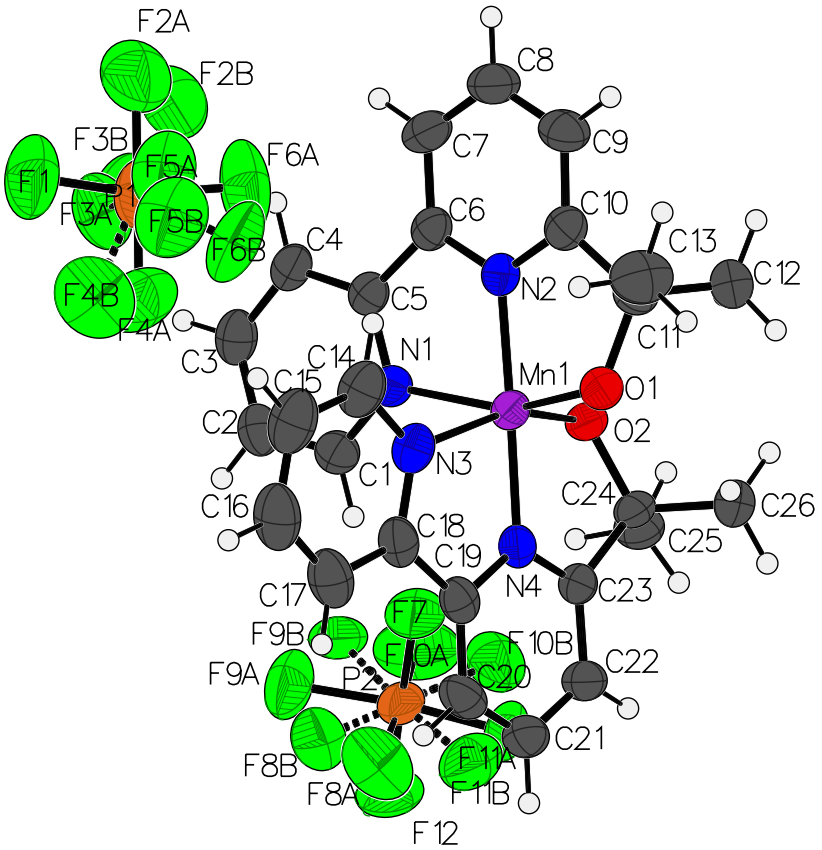

Figure S20. The complete numbering scheme of **4** with 50% thermal ellipsoid probability levels. The hydrogen, fluorine and phosphorus atoms are shown as circles for clarity. The dashed bonds highlight disordered positions.

Table S6. Crystal data and structure refinement for **4**.

Identification code	007-16120	
Empirical formula	C26 H26 F12 Mn N4 O2 P2	
Formula weight	771.39	
Temperature	93(2) K	
Wavelength	1.54178 Å	
Crystal system	Triclinic	
Space group	P-1	
Unit cell dimensions	a = 11.9537(8) Å	α = 116.911(4)°.
	b = 12.4244(9) Å	β = 102.591(7)°.
	c = 12.5022(13) Å	γ = 97.214(5)°.
Volume	1561.3(2) $Å^3$	
Z	2	
Density (calculated)	1.641 Mg/m^3	
Absorption coefficient	5.379 mm^{-1}	
F(000)	778	
Crystal size	0.050 x 0.010 x 0.010 mm^3	
Theta range for data collection	3.921 to 68.280°.	
Index ranges	-14<=h<=14, -14<=k<=14, -14<=l<=14	
Reflections collected	55551	
Independent reflections	5518 [R(int) = 0.1839]	
Completeness to theta = 67.679°	97.6 %	
Absorption correction	Semi-empirical from equivalents	
Max. and min. transmission	1.000 and 0.703	
Refinement method	Full-matrix least-squares on F^2	
Data / restraints / parameters	5518 / 225 / 511	
Goodness-of-fit on F^2	0.947	
Final R indices [I>2sigma(I)]	R1 = 0.0662, wR2 = 0.1671	
R indices (all data)	R1 = 0.0929, wR2 = 0.1805	
Extinction coefficient	0.0040(5)	
Largest diff. peak and hole	0.562 and -0.579 e.$Å^{-3}$	

3. References:

[1] H. Chen, R. Tagore, S. Das, C. Incarvito, J. W. Faller, R. H Crabtree, G. W. Brudvig, *Inorg. Chem.* **2005**, *44,* 7661–7670.

[2] M. N. Collomb, A. Deronzier, A. Richardot J. Pecaut, *New J. Chem.* **1999**, *23,* 351–353.

[3] H. Chen, J. W. Faller, R. H. Crabtree, G. W. Brudvig, *J. Am. Chem. Soc.* **2004**, *126,* 7345–7349.

[4] H. Yamazaki, S. Igarashi, T. Nagata, M. Yagi, *Inorg. Chem.* **2012**, *51,* 1530–1539.